# Meshless BEM and overlapping Schwarz preconditioners for exterior problems on spheroids


| | |
|---|---|
| Journal: | *Studia Geophysica et Geodaetica* |
| Manuscript ID: | SGEG-2010-0055 |
| Manuscript Type: | Original Article |
| Date Submitted by the Author: | 28-Jun-2010 |


| | |
|---|---|
| Complete List of Authors: | Costea, Adrian; Leibniz University Hanover, Institute for Applied Mathematics<br>Stephan, Ernst; Leibniz University Hanover, Institute for Applied Mathematics<br>LeGia, Quoc; University of New South Wales, School of Mathematics and Statistics<br>Tran, Thanh; University of New South Wales, School of Mathematics and Statistics |


| | |
|---|---|
| Keywords: | Boundary integral equations, meshless methods, spheroids, overlapping Schwarz, domain decomposition |

# Meshless BEM and overlapping Schwarz preconditioners for exterior problems on spheroids

A. Costea * Q.T. Le Gia † E.P. Stephan* T. Tran †



**Abstract**

We consider the exterior Neumann problem of the Laplacian with boundary condition on a prolate spheroid. We propose to use spherical radial basis functions in the solution of the boundary integral equation arising from the Dirichlet-to-Neumann map. Our meshless approach with radial basis functions is particularly suitable for handling scattered satellite data. We also propose a preconditioning technique based on an overlapping domain decomposition method to deal with ill-conditioned matrices arising from the approximation problem.

Here we report from Le Gia et al. (2010), Costea et al. (Solution to the Neumann problem exterior to an oblate spheroid by radial basis functions, in preparation, 2010) on a meshless method with radial basis functions for the Neumann problem for the Laplacian exterior to an oblate or a prolate spheroid. In geophysical applications, see Freeden et al. (1998) and Krumm et al. (2003), one is interested in such exterior Neumann problems where the orbits of satellites are located on spheroids. The satellites create data which amount to boundary conditions given in scattered points. A key tool of our approach is the use of the Dirichlet-to-Neumann map which directly converts the bounday value problem into a pseudodifferential equation on the spheroid. This integral equation is then handled with Fourier techniques by expansion into appropriate spherical harmonics. In Huang and Yu (2009) this pseudodifferential equation was solved numerically with

*Institut für Angewandte Mathematik and QUEST (Centre for Quantum Engineering and Space-Time Research), Leibniz Universität Hannover, Welfengarten 1, 30167 Hannover, Germany. Email: costea@ifam.uni-hannover.de, stephan@ifam.uni-hannover.de

†School of Mathematics and Statistics, University of New South Wales, Sydney, NSW 2052, Australia. Email: qlegia@unsw.edu.au, Thanh.Tran@unsw.edu.au,

standard boundary elements on a regular grid on the angular domain of the spherical coordinates. Our approach uses spherical radial basis functions (SRBF's) instead, allowing for better handling of scattered data. The error analysis for the meshless method with radial basis functions on the sphere as done in Tran et al. (2009) has been extended to spheroids in Le Gia et al. (2010) and Costea et al. (Solution to the Neumann problem exterior to an oblate spheroid by radial basis functions, in preparation, 2010). Again the smooth solution of the pseudodifferential equation can be approximated with high convergence rates by the Galerkin solution consisting of radial basis functions. The numerical solution is obtained by an appropriate implementation of the prolate and oblate spheroidal harmonics and by truncating the resulting infinite dimensional discrete Galerkin system.

We present numerical results of our meshless boundary element method for points from an equal area partitioning algorithm, so-called Saff points (Fig.1), and for scattered data points from satellite observations (Fig.2). Furthermore we present iteration numbers for the conjugate gradient method applied to solve the discrete systems in case of scattered data. We list the iteration numbers for the preconditioned conjugate gradient method when an overlapping additive Schwarz method is used as preconditioner. For both oblate and prolate spheroids we obtain only mildly growing iteration numbers for the overlapping additive Schwarz method. This technique was firstly analysed for pseudodifferential equations on the sphere in Tran et al. (2010) .

Let $\Gamma_0 = \{(x_1, x_2, x_3) \in \mathbb{R}^3 : \frac{x_1^2+x_2^2}{b^2} + \frac{x_3^2}{a^2} = 1,\ a > b > 0\}$ be a prolate spheroid and $\Omega^c$ be the unbounded domain outside the boundary $\Gamma_0$. We consider the exterior Neumann problem: given $g$ defined on $\Gamma_0$, find $U$ defined on $\Omega^c$ satisfying

$$\begin{cases} \Delta U = 0 & \text{in} \quad \Omega^c \\ \partial_\nu U = g & \text{on} \quad \Gamma_0 \\ U(\boldsymbol{x}) = O(||\boldsymbol{x}||^{-1}) & \text{as} \quad ||\boldsymbol{x}|| \to \infty \end{cases} \tag{0.1}$$

where $||\boldsymbol{x}||$ denotes the Euclidean norm of $\boldsymbol{x}$ and $\nu$ denotes the unit outward normal vector on $\Gamma_0$.
The solution is given by the series

$$U(\mu, \theta, \varphi) = \sum_{n=0}^{\infty} \sum_{m=-n}^{n} \frac{Q_n^m(\cosh \mu)}{Q_n^m(\cosh \mu_0)} \widehat{u}_{nm} Y_{nm}(\theta, \varphi), \quad \mu \geq \mu_0 > 0. \tag{0.2}$$

where $(\mu, \theta, \varphi)$ denote the prolate spheroidal coordinates of $\boldsymbol{x} \in \Gamma_0$ (Huang and Yu (2009)). Here $Q_n^m$ are the associated Legendre functions of second kind,

$Y_{nm}$ the spherical harmonics of degree $n$, and $\hat{u}_{nm}$ the expansion coefficients. In Huang and Yu (2009) it is shown that (0.1) is equivalent to

$$\mathcal{K}u = g \quad \text{on} \quad \Gamma_0 \tag{0.3}$$

with the Dirichlet-to-Neumann map (Steklov-Poincaré operator) $\mathcal{K}$. Its weak formulation is: Find $u \in H^{1/2}(\Gamma_0)$ satisfying

$$D(u,v) := \int_{\Gamma_0} (\mathcal{K}u)v\, ds = \int_{\Gamma_0} gv\, ds \quad \forall v \in H^{1/2}(\Gamma_0) \tag{0.4}$$

$$\text{with} \quad D(u,v) = f_0 \sum_{n=0}^{\infty} \sum_{m=-n}^{n} H_n^m(\cosh \mu_0)\widehat{u}_{nm}\widehat{v}_{nm}^*, \tag{0.5}$$

$$\text{where} \quad H_n^m(x) := -\frac{(x^2-1)dQ_n^m(x)/dx}{Q_n^m(x)}. \tag{0.6}$$

Here we recall that the Sobolev space $H^s(\Gamma_0)$ is defined by

$$u \in H^s(\Gamma_0), s \in \mathbb{R} \Longleftrightarrow \|u\|^2_{H^s(\Gamma_0)} := \sum_{n=0}^{\infty} \sum_{m=-n}^{n} (1+n^2)^s |\hat{u}_{nm}|^2 < \infty \tag{0.7}$$

**Proposition**: *There exists a unique solution for the variational problem* (0.4). This is due to the Lax-Milgram theorem since $D(\cdot,\cdot)$ is continuous and coercive on the Sobolev space $H^{1/2}(\Gamma_0)$ and the right hand side in(0.4) defines a continuous linear functional on $H^{1/2}(\Gamma_0)$. The approximate solution to (0.4) is sought in a finite dimensional subspace of $H^{1/2}(\Gamma_0)$. In order to use SRBFs we take the bijection $\omega : \Gamma_0 \to \mathbb{S}^2$ (where $\mathbb{S}^2$ is the unit sphere in $\mathbb{R}^3$)

$$\omega(\boldsymbol{x}) = (\sin\theta\cos\varphi, \sin\theta\sin\varphi, \cos\theta), \tag{0.8}$$

and we define a reproducing kernel on $\Gamma_0$ as

$$\Psi(\boldsymbol{x}, \boldsymbol{x}') = \Phi(\omega(\boldsymbol{x}), \omega(\boldsymbol{x}')), \quad \boldsymbol{x}, \boldsymbol{x}' \in \Gamma_0, \tag{0.9}$$

where $\Phi$ is defined via a univariate function $\phi : [-1,1] \to \mathbb{R}$ by $\Phi(\boldsymbol{y}, \boldsymbol{z}) = \phi(\boldsymbol{y} \cdot \boldsymbol{z}) \quad \forall \boldsymbol{y}, \boldsymbol{z} \in \mathbb{S}^2$ (see Schoenberg (1942) and Xu and Cheney (1992)). Here $\phi$ has a series expansion in terms of Legendre polynomials $P_n$ of degree $n$, as

$$\phi(t) = \frac{1}{4\pi} \sum_{n=0}^{\infty} (2n+1)\hat{\phi}(n)P_n(t) \quad \text{with} \quad \hat{\phi}(n) = 2\pi \int_{-1}^{+1} \phi(t)P_n(t)dt. \tag{0.10}$$

The kernel $\Psi$ can be expanded into a series of spherical harmonics as

$$\Psi(\boldsymbol{x},\boldsymbol{x}') = \sum_{n=0}^{\infty}\sum_{m=-n}^{n} \hat{\phi}(n) Y_{nm}(\omega(\boldsymbol{x}))Y^*_{nm}(\omega(\boldsymbol{x}')) \tag{0.11}$$

where we choose $\phi$ such that

$$\hat{\phi}(n) \simeq (1+n^2)^{-\tau} \quad \text{for some} \quad \tau > 0. \tag{0.12}$$

Given a set of scattered data points $X = \{\boldsymbol{x}_1, ..., \boldsymbol{x}_M\} \subset \Gamma_0$, we take

$$V^\tau := \text{span}\{\Psi_j := \Psi(\boldsymbol{x}_j, \cdot) : \boldsymbol{x}_j \in X\}.$$

Now, the solution of (0.4) is approximated by $u_X \in V^\tau$ satisfying the Galerkin equation

$$D(u_X, v) = \int_{\Gamma_0} gv\, ds \quad \forall v \in V^\tau. \tag{0.13}$$

To this end we have to solve a linear system

$$A\boldsymbol{c} = \boldsymbol{g} \tag{0.14}$$

where A is a matrix with entries $A_{i,j} = D(\Psi_i, \Psi_j),\ i,j = 1, ..., M$, and $\boldsymbol{g}$ is a vector with entries $g_j = \int_{\Gamma_0} g\Psi_j\, ds, \quad j = 1, .., M$. Using (0.5) and (0.11) we can write

$$A_{i,j} = f_0 \sum_{n=0}^{\infty}\sum_{m=-n}^{n} [\hat{\phi}(n)]^2 H_n^m(\cosh\mu_0) Y_{nm}(\omega(\boldsymbol{x}_i))Y^*_{nm}(\omega(\boldsymbol{x}_j)). \tag{0.15}$$

Further let $N$ denote the number of the series terms of the truncated matrix element $A^N_{i,j}$. We compute the actual Galerkin approximation $u_X$ by solving (0.14) with the Galerkin matrix $A^N$ obtained via the truncated entries $A^N_{i,j}$.

Let $Y = \{\boldsymbol{y}_1, ..., \boldsymbol{y}_M\}$ be the image of $X$ under the map $\omega$, i.e. $\boldsymbol{y}_j = \omega(\boldsymbol{x}_j)$ for $j = 1, ..., M$. As $Y$ is a set of scattered points on $\mathbb{S}^2$, we define the mesh norm $h_Y$ of $Y$ as usual as $h_Y = \sup_{\boldsymbol{y}\in\mathbb{S}^2} \min_{\boldsymbol{y}_j\in Y} \cos^{-1}(\boldsymbol{y}\cdot\boldsymbol{y}_j)$.

**Proposition (Le Gia et al. (2010))**: *For a prolate spheroid and truncation number $N$ chosen sufficiently large there holds the quasioptimal error estimate for the difference between the exact solution $u \in H^s(\Gamma_0)$ of (0.4) and the Galerkin solution $u_X \in V^\tau$, $2\tau > s+1$ of (0.13)*

$$\|u - u_X\|_{H^{1/2}(\Gamma_0)} \leq Ch_Y^{s-1/2}, \tag{0.16}$$

*where the constant $C$ is independent of the set $X$ used to define $\Psi_j$, but may depend on $N$.* (For the corresponding result for the oblate spheroid see Costea et al. (Solution to the Neumann problem exterior to an oblate spheroid by radial basis functions, in preparation, 2010).)

Our numerical experiments plotted in (Fig. 3) for the mesh of Saff points show these predicted convergence rates $\alpha$, namely $\alpha = 2.5$ for $Pm = 0(\tau = 1.5)$,$\alpha = 4.5$ for $Pm = 1(\tau = 2.5)$,$\alpha = 6.5$ for $Pm = 2(\tau = 3.5)$, cf. Table 2.

To compute the entries $A_{ij}$ of the stiffness matrix given in (0.15), we need to compute the spherical harmonics $Y_{nm}$ and the functions $H_n^m$.
The term $H_n^m(\cosh\mu_0)$ in the entry $A_{i,j}$ of the stiffness matrix (see (0.15) and (0.6)) can be computed by using the relation

$$H_n^m(x) = -(n-m+1)Q_{n+1}^m(x)/Q_n^m(x) + (n+1)x, m = 0, \dots, n;\ n = 0, 1, \dots \quad (0.17)$$

For negative values of $m$ we use the relation $H_n^m(x) = H_n^{-m}(x)$.

The right hand side terms $g_j$ are computed by using the Fourier coefficients of $g$ and $\Psi_j$ and Parseval's identity.
We use different kernels $\Psi(\boldsymbol{x}, \boldsymbol{x}') = \Phi(\omega(\boldsymbol{x}), \omega(\boldsymbol{x}'))$ in our numerical experiments, where the functions $\Phi$ are restrictions to the sphere of two different classes of positive definite RBFs defined by Matérn and Wendland functions.

The Matérn functions (or Sobolev splines) were introduced for statistical applications in Matérn (1986). They are defined by

$$\phi_\nu(r) = \frac{2^{\nu-1}}{\Gamma(\nu)} r^{\nu-3/2} K_{\nu-3/2}(r), \quad \nu > 3/2, \quad (0.18)$$

where $K_\nu$ is the $K$-Bessel function of order $\nu$. In $\mathbb{R}^3$, the Fourier transform of $\phi$ decays like $\widehat{\phi}(\xi) \sim (1 + \|\xi\|_2^2)^{-\nu}$. The Matérn kernels used in our experiments are listed in Table 1. When restricting to the sphere, the native space associated with the kernel $\Phi(\boldsymbol{y}, \boldsymbol{z}) := \phi_\nu(\sqrt{2 - 2\boldsymbol{y}\cdot\boldsymbol{z}})$ is the Sobolev space $H^{\nu-1/2}(\mathbb{S}^2)$, see Narcowich et al. (2007).

The Wendland functions discussed in Wendland (2005) are positive definite functions with compact support. For arbitrary $\boldsymbol{y}, \boldsymbol{z} \in \mathbb{S}^2$, $\Phi(\boldsymbol{y}, \boldsymbol{z}) = \rho_m(\sqrt{2 - 2\boldsymbol{y}\cdot\boldsymbol{z}})$ with $\rho_m$ being locally supported radial basis functions defined by Wendland; see Table 2. In this case (0.12) holds for $\tau = m + 3/2$ see Narcowich and Ward (2002) .

**Example 1**: Problem (0.1) with **prolate spheroid** $\Gamma_0$ ($f_0 = 4$, $\mu_0 = 1$), Neumann condition and exact solution

$$g(\mu, \theta, \varphi) = -\frac{\sqrt{2}\sin 2\theta \cos\varphi(7 - 3\cosh 4\mu + 4\cosh 2\mu \cos 2\theta)}{4f_0^4\sqrt{\cosh^2\mu - \cos^2\theta}(\cosh 2\mu + \cos 2\theta)^{7/2}} \quad (0.19)$$

$$U(\mu,\theta,\varphi) = \frac{\sqrt{2}\sinh 2\mu \sin 2\theta \cos\varphi}{2f_0^3(\cosh 2\mu + \cos 2\theta)^{5/2}}. \tag{0.20}$$

Let $e := u - u_X$ where $u(\theta,\varphi) = U(\mu_0,\theta,\varphi)$, solves (0.4) and $u_X$ solves (0.13) with truncation number $N_{trunc} = 100$.

We compute $\|e\|_{L^2(\Gamma_0)}$ and $\|e\|_{H^{1/2}(\Gamma_0)}$ approximately by $N_{max} = 120$

$$\|e\|_{L^2(\Gamma_0)} \approx \left(\sum_{n=0}^{N_{max}} \sum_{m=-n}^{n} |\widehat{u_X}_{nm} - \hat{u}_{nm}|^2\right)^{1/2} \tag{0.21}$$

and

$$\|e\|_{H^{1/2}(\Gamma_0)} \approx \left(\sum_{n=0}^{N_{max}} (1+n^2)^{1/2} \sum_{m=-n}^{n} |\widehat{u_X}_{nm} - \hat{u}_{nm}|^2\right)^{1/2} \tag{0.22}$$

with $\widehat{u_X}_{nm} = \sum_{i=1}^{M} \hat{\phi}(n) c_i Y_{nm}(\omega(\boldsymbol{x}_i))$ and $\hat{u}_{nm}$ is computed by an appropriate quadrature formula as shown in Driscoll and Healy (1994).

Table 3 gives the errors in the $L^2(\Gamma_0)$ and $H^{1/2}(\Gamma_0)$ norms for scattered points. The matrix is ill conditioned and a preconditioner is required.

The symbol of the operator $\mathcal{K}$ behaves like $(n^2+1)^{1/2}$, see Le Gia et al. (2010). Hence $\mathcal{K}$ is a pseudodifferential operator of order 1. This allows us to extend our analysis discussed in Tran et al. (2010) for the overlapping Schwarz preconditioner on the sphere to the prolate spheroid.

The preconditioner is defined by the additive Schwarz operator, using a subspace decomposition of $V^\tau$ as $V^\tau = V_0 + \ldots + V_J$.
These subspaces $V_j$, $j = 0,\ldots,J$, are defined from a decomposition of the set $Y$ into overlapping subsets $Y_j$, $j = 0,\ldots,J$. These subsets are generated by the following algorithm:

Select $\tilde{\alpha} \in (0,\pi/3)$, $\quad \beta \in (0,\pi]$;
$\boldsymbol{p}_1 = \boldsymbol{y}_1 \in Y$;
$Y_0 := \{\boldsymbol{p}_1\}$;
$Y_1 := \{\boldsymbol{y} \in Y : \cos^{-1}(\boldsymbol{y}\cdot\boldsymbol{p}_1) \le \tilde{\alpha}\}$;
$J = 1,\ k = 1$;
**while** $Y_1 \cup \cdots \cup Y_k \ne Y$ **do**
  $k = k+1$;
  $\boldsymbol{p}_k$ is chosen from $Y \setminus Y_0$ such that $\cos^{-1}(\boldsymbol{p}_{k-1}\cdot\boldsymbol{p}_k) \ge \beta$;
  $Y_0 := Y_0 \cup \{\boldsymbol{p}_k\}$;
  $Y_k := \{\boldsymbol{y} \in Y : \cos^{-1}(\boldsymbol{y}\cdot\boldsymbol{p}_k) \le \tilde{\alpha}\}$
**end**
$J = k$.

Each set $Y_k$ is a collection of points inside a spherical cap of radius $\tilde{\alpha}$ centered at $\boldsymbol{p}_k$. These sets define subdomains on the prolate spheroid.

The centers $\boldsymbol{p}_k$ are chosen so that the geodesic distance between two successive centers is not less than $\beta$, see Le Gia et al. (2010) This is to ensure that finally all points are considered, and thus the algorithm terminates. The set $Y_0$ serves as the coarse mesh in domain decomposition methods for finite element approximations. This set defines the space $V_0$ which provides global communication of data.

Table 4 shows the corresponding numbers of iteration of the preconditioned conjugate gradient method (PCG) with an overlapping additive Schwarz preconditioner; stopping criteria in both cases is relative tolerance $\leq 10^{-8}$. Errors of the same order as in the non-preconditioned case are obtained but PCG needs much smaller iteration numbers.(CPU: computational times in seconds, ITER: numbers of iterations)

In Costea et al. (Solution to the Neumann problem exterior to an oblate spheroid by radial basis functions, in preparation, 2010) we have analysed the foregoing meshless boundary element method for an oblate spheroid. We obtain similar results both with respect to convergence of the meshless Galerkin solution as well as the behaviour of the iteration number of PCG. For brevity we present only some numerical results.

**Example 2**: Problem (0.1) with **oblate spheroid** $\Gamma_0$ (see also Costea et al. (Solution to the Neumann problem exterior to an oblate spheroid by radial basis functions, in preparation, 2010)), with Neumann condition and exact solution

$$g = -\frac{\sinh\mu\sin\theta\cos\varphi(2\cosh^2\mu+\cos^2\theta)}{f_0^2(\cosh^2\mu-\cos^2\theta)^{\frac{5}{2}}}, \quad U = \frac{\cosh\mu\sin\theta\cos\varphi}{f_0^2(\cosh^2\mu-\cos^2\theta)^{\frac{3}{2}}}. \quad (0.23)$$

Figure 4 shows the experimental orders of convergence (EOC) for the errors in the $H^{1/2}(\Gamma_0)$-norm (energy norm) when Saff points and Wendland's kernels are used, for the prolate (Pm) and oblate (Om) spheroid. Figure 5 shows the corresponding results when Matérn kernels are used for the prolate (Example 1) and oblate (Example 2) spheroid.

Tables 5 and 6 give the errors in the $L^2(\Gamma_0)$ and $H^{1/2}(\Gamma_0)$ norms and the iteration numbers for CG and PCG for scattered points for Example 2 (stopping criteria in both cases is relative tolerance $\leq 10^{-10}$). We observe for the oblate spheroid that the errors of the meshless boundary element method and the performance of the PCG with overlapping Schwarz preconditioner behave as in the case of the prolate spheroid.

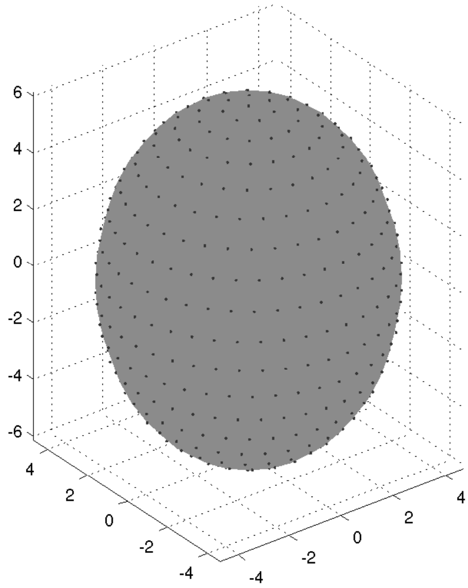


Figure 1: Image of Saff points on the prolate spheroid

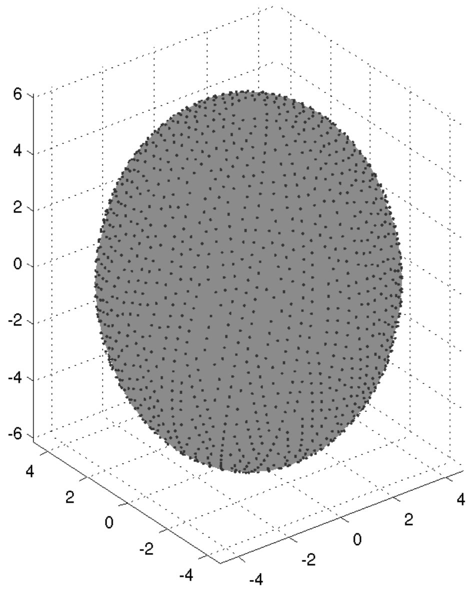


Figure 2: Image of satellite points on the prolate spheroid

| $\nu$ | $\phi_\nu(r)$ | $\tau$ |
|---|---|---|
| 2 | $e^{-r}$ | 1.5 |
| 3 | $e^{-r}(1+r)$ | 2.5 |

Table 1: Matérn's RBFs

| $m$ | $\rho_m(r)$ | $\tau$ |
|---|---|---|
| 0 | $(1-r)_+^2$ | 1.5 |
| 1 | $(1-r)_+^4(4r+1)$ | 2.5 |
| 2 | $(1-r)_+^6(35r^2+18r+3)$ | 3.5 |

Table 2: Wendland's RBFs

| $m$ | $M$ | $q_Y$ | $\|e\|_{L^2(\Gamma_0)}$ | $\|e\|_{H^{1/2}(\Gamma_0)}$ | CPU | ITER |
|---|---|---|---|---|---|---|
| 0 | 2133 | $\pi/100$ | 1.08971E-6 | 7.79793E-6 | 19.2 | 1124 |
| | 7763 | $\pi/200$ | 2.15172E-7 | 1.81600E-6 | 1592.3 | 7518 |
| 1 | 2133 | $\pi/100$ | 3.76100E-8 | 2.54359E-7 | 102 | 7737 |
| | 7763 | $\pi/200$ | 1.03461E-8 | 6.99365E-8 | 620.6 | 4059 |

Table 3: Errors with scattered points from MAGSAT, using CG, $\rho_m(r)$, Ex.1

| $m$ | $M$ | $\cos\tilde{\alpha}$ | $\cos\beta$ | $J$ | CPU | ITER | $\|e\|_{L^2(\Gamma_0)}$ |
|---|---|---|---|---|---|---|---|
| 0 | 2133 | 0.90 | -0.01 | 42 | 4.4 | 68 | 0.11045E-5 |
| | 2133 | 0.80 | -0.66 | 22 | 4.6 | 45 | 0.11045E-5 |
| | 2133 | 0.70 | -0.78 | 17 | 5.6 | 36 | 0.11045E-5 |
| | 2133 | 0.60 | -0.69 | 11 | 4.1 | 22 | 0.11045E-5 |
| | 7763 | 0.97 | 0.63 | 140 | 176.1 | 226 | 0.24240E-6 |
| | 7763 | 0.90 | -0.46 | 48 | 133.6 | 85 | 0.24247E-6 |
| | 7763 | 0.80 | -0.76 | 23 | 162.1 | 59 | 0.24239E-6 |
| | 7763 | 0.70 | -0.84 | 17 | 238.2 | 51 | 0.24239E-6 |
| 1 | 2133 | 0.90 | -0.01 | 42 | 10.9 | 251 | 0.36969E-7 |
| | 2133 | 0.80 | -0.66 | 22 | 6.1 | 95 | 0.36969E-7 |
| | 2133 | 0.70 | -0.78 | 17 | 7.9 | 75 | 0.36969E-7 |
| | 2133 | 0.60 | -0.69 | 11 | 2.8 | 22 | 0.36969E-7 |
| | 7763 | 0.97 | 0.63 | 140 | 323.3 | 738 | 0.36654E-8 |
| | 7763 | 0.90 | -0.46 | 48 | 104.5 | 147 | 0.42327E-8 |
| | 7763 | 0.80 | -0.76 | 23 | 55.8 | 40 | 0.47790E-8 |
| | 7763 | 0.70 | -0.84 | 17 | 154.8 | 60 | 0.35058E-8 |

Table 4: Errors with scattered points from MAGSAT, for PCG, $\rho_m(r)$, Ex.1

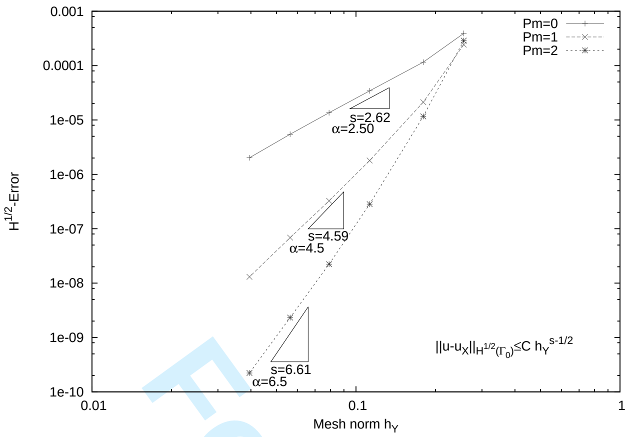


Figure 3: Log-log plot for $H^{1/2}(\Gamma_0)$ errors using Wendland RBFs $\rho_m(r)$ for the prolate spheroid

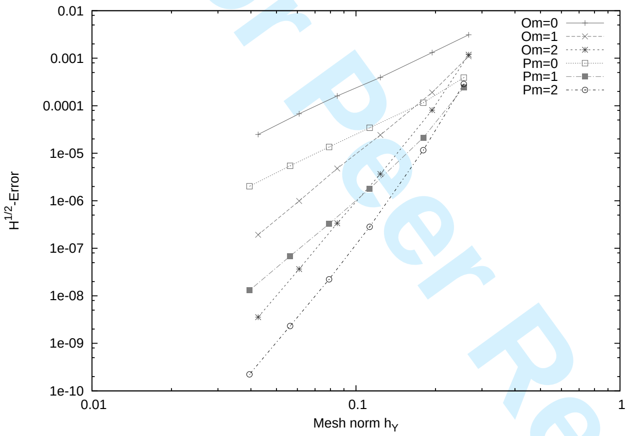


Figure 4: Log-log plot for $H^{1/2}(\Gamma_0)$ errors using Wendland RBFs $\rho_m(r)$ (Saff points) for the prolate (Pm) and oblate spheroid (Om)

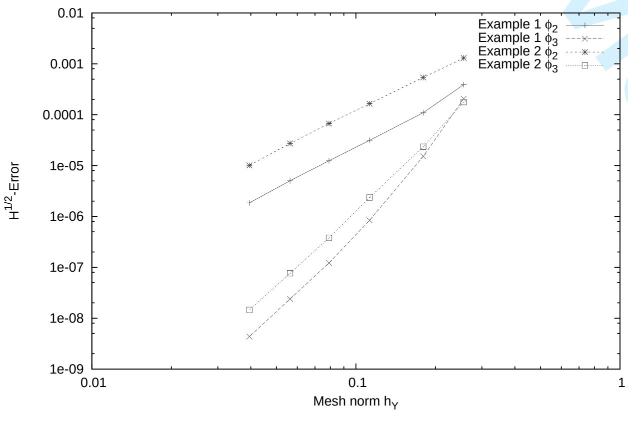


Figure 5: Log-log plot for $H^{1/2}(\Gamma_0)$ errors using Matérn RBFs $\phi_\nu(r)$ (Saff points) for the prolate (Ex.1) and oblate spheroid (Ex.2)

| $M$ | $q_Y$ | $\|e\|_{L^2(\Gamma_0)}$ | $\|e\|_{H^{1/2}(\Gamma_0)}$ | ITER | CPU |
|---|---|---|---|---|---|
| 3470 | $\pi/140$ | 6.25503E-006 | 5.01114E-005 | 2809 | 234.6 |
| 7763 | $\pi/200$ | 2.41695E-006 | 2.13257E-005 | 27064 | 13323.7 |
| 10443 | $\pi/240$ | 1.87142E-006 | 1.62031E-005 | 30931 | 17361.9 |

Table 5: Errors with scattered points from MAGSAT, using CG, $\rho_0(r)$, Ex.2

| $M$ | $\cos\tilde{\alpha}$ | $\cos\beta$ | $\|e\|_{L^2(\Gamma_0)}$ | $\|e\|_{H^{1/2}(\Gamma_0)}$ | ITER | CPU |
|---|---|---|---|---|---|---|
| 3470 | 0.90 | -.16 | 6.25503E-006 | 5.01114E-005 | 71 | 10.7 |
| 3470 | 0.80 | -.55 | 6.25503E-006 | 5.01114E-005 | 44 | 11.6 |
| 3470 | 0.70 | -.80 | 6.25503E-006 | 5.01114E-005 | 32 | 12.7 |
| 3470 | 0.60 | -.86 | 6.25503E-006 | 5.01114E-005 | 35 | 22.3 |
| 7763 | 0.97 | 0.63 | 2.41695E-006 | 2.13257E-005 | 227 | 103.4 |
| 7763 | 0.95 | -.08 | 2.41695E-006 | 2.13257E-005 | 168 | 109.1 |
| 7763 | 0.90 | -.46 | 2.41695E-006 | 2.13257E-005 | 87 | 85.4 |
| 7763 | 0.85 | -.56 | 2.41695E-006 | 2.13257E-005 | 65 | 103.0 |
| 10443 | 0.98 | 0.95 | 1.87142E-006 | 1.62031E-005 | 310 | 309.1 |
| 10443 | 0.97 | 0.69 | 1.87142E-006 | 1.62031E-005 | 156 | 160.2 |
| 10443 | 0.96 | 0.08 | 1.87142E-006 | 1.62031E-005 | 189 | 227.5 |
| 10443 | 0.95 | -.07 | 1.87142E-006 | 1.62031E-005 | 120 | 156.4 |

Table 6: Errors with scattered points from MAGSAT, for PCG, $\rho_0(r)$, Ex.2

## References

Driscoll, James R. and Healy, Jr., Dennis M. 1994. Computing Fourier transforms and convolutions on the 2-sphere. *Adv. in Appl. Math.*, 15(2):202–250.

Freeden, W., Gervens, T., and Schreiner, M. 1998. *Constructive approximation on the sphere*. Numerical Mathematics and Scientific Computation. The Clarendon Press Oxford University Press, New York. With applications to geomathematics.

Grafarend, E. W., Krumm, F. W., and Schwarze, V. 2003. *Geodesy: the Challenge of the 3rd Millennium*. Springer, Berlin.

Huang, H. and Yu, D. 2009. The ellipsoid artificial boundary method for three-dimensional unbounded domains. *J. Comput. Math.*, 27(2-3):196–214.

Le Gia, Q. T., Tran, T., and Stephan, E. P. 2010. Solution to the Neumann problem exterior to a prolate spheroid by radial basis functions. *Adv. Comput. Math.* DOI 10.1007/s10444-010-9145-4.

Matérn, B. 1986. *Spatial variation*, volume 36 of *Lecture Notes in Statistics*. Springer-Verlag, Berlin, second edition.

Narcowich, F. J., Sun, X., and Ward, J. D. 2007. Approximation power of RBFs and their associated SBFs: a connection. *Adv. Comput. Math.*, 27(1):107–124.

Narcowich, F. J. and Ward, J. D. 2002. Scattered data interpolation on spheres: error estimates and locally supported basis functions. *SIAM J. Math. Anal.*, 33(6):1393–1410 (electronic).

Schoenberg, I. J. 1942. Positive definite functions on spheres. *Duke Math. J.*, 9:96–108.

Tran, T., Le Gia, Q. T., Sloan, I. H., and Stephan, E. P. 2009. Boundary integral equations on the sphere with radial basis functions: error analysis. *Appl. Numer. Math.*, 59(11):2857–2871.

Tran, T., Le Gia, Q. T., Sloan, I. H., and Stephan, E. P. 2010. Preconditioners for pseudodifferential equations on the sphere with radial basis functions. *Numer. Mathematik*, 115(1):141–163.

Wendland, H. 2005. *Scattered data approximation*, volume 17 of *Cambridge Monographs on Applied and Computational Mathematics*. Cambridge University Press, Cambridge.

Xu, Y. and Cheney, E. W. 1992. Strictly positive definite functions on spheres. *Proc. Amer. Math. Soc.*, 116(4):977–981.